

38th Annual Graduate Student Colloquium



Alaskan Range, Alaska submitted by Tyrone Rooney

**Sponsored by the
Department of Geosciences
April 24-28, 2006**

38th Annual Graduate Student Colloquium

Sponsored by the
Department of Geosciences
April 24-28, 2006

The Graduate Student Colloquium is a forum where students present their research or research proposal to faculty, friends, and peers. The Colloquium is hosted by the Department of Geosciences and is open to graduate students involved in geoscience research. The colloquium format stimulates research discussion, allows students to practice for national meetings, and helps students improve their speaking skills. The Colloquium helps both the Department of Geosciences and Penn State to maintain and strengthen their reputations at national meetings for giving high quality talks and posters with visual appeal.

Schedule of Events:

Opening Reception	10:00 April 24th	EMS Museum, Ground Floor Deike
Poster Session	1:00-3:00 April 24th	EMS Museum, Ground Floor Deike
Poster Viewing	April 27th-May 4th	EMS Museum, Ground Floor Deike
Talk Session 1	1:00-3:00 April 24th	541 Deike
Talk Session 2	9:00-12:00 April 26th	541 Deike
Talk Session 3	1:00-3:15 April 26th	541 Deike
Talk Session 4	9:00-12:00 April 27th	541 Deike
Entropy	6:00-??? April 28th	VFW Hall

The Graduate Colloquium Committee wishes to thank the students for sharing their work and the faculty for giving constructive advice. The Committee also wishes to thank the Shell People Services division of Shell Oil Company, Chevron, and the Department of Geosciences for their donations of prize money and their generous financial support.



Committee Members 2006: Jennifer Nemitz (chair), David Bevacqua, Doug Edmonds, Bryn Kimball, Angela "Mouse" Larson, Vikki Miller, Matt O'Donnell, Andy Rathbun, Dave Vacco, Andy Wall, and Paul Winberry

ORAL PRESENTATION SCHEDULE - MONDAY AFTERNOON

<u>Time</u>	<u>Presenter</u>	<u>Advisor</u>	<u>Title</u>
1:00	Matthew O'Donnell	Mark Patzkowsky	A FACIES-PRESERVATION MODEL OF DIVERSITY
1:15	Louanne Christopher	Peter Flemings	1D COMPACTION FLOW MODELING OF URSA CANYON
1:30	Daniel Hummer	Peter Heaney	AQUEOUS NUCLEATION AND GROWTH OF TITANIUM OXIDES USING TIME-RESOLVED SYNCHROTRON X-RAY DIFFRACTION
1:45	James Moran	Katherine Freeman, Christopher House	OXYGEN TOLERANCE IN 'STRICTLY' ANAEROBIC METHANOGENS
2:00	BREAK		
2:15	Alexis Navarre	Susan Brantley	BASALT WEATHERING RATES ACROSS SCALES
2:30	Jennifer Nemitz	Richard Parizek	ARE WE DRUGGING OUR DRINKING WATER? OCCURRENCE, FATE, AND TRANSPORT OF PHARMACEUTICALS AT PENN STATE'S LIVING FILTER
2:45	Leo Peters	Sridhar Anandakrishnan	BASAL CONDITIONS NEAR THE ONSET OF ICE STREAM D, WEST ANTARCTICA

A FACIES-PRESERVATION MODEL OF DIVERSITY

Matthew O'Donnell

Advisor: Mark Patzkowsky

Pre-Comps Talk

A long-standing debate in palaeobiology is how well preserved diversity reflects true past diversity levels. The first tabulations of marine diversity showed a striking correlation to amounts of rock volume preserved through time, suggesting that preservational processes have biased the record of preserved diversity. These studies looked at preservation at a global level, but since recent work has shown that global diversity is composed of many varying smaller-scale patterns, the effects of preservation on diversity should be examined at the level of regions or environments. For example, since taxonomic rates vary among marine facies, differential preservation among these facies will affect apparent diversity trends and rate estimates.

We present a null model to predict the effect of differential preservation among facies on preserved rates of origination and extinction. The model is based on the onshore-offshore diversity model of Sepkoski (1991) with the addition of preservation rates and tabulating taxonomic rates by facies. The model consists of a matrix representing a facies gradient from nearshore to offshore for a specified number of time steps representing one million years each. Equal and constant taxonomic rates (origination and extinction) maintain constant diversity within each facies for the whole model run. Preservation rate may change independently of time and rates in other facies. Changing preservation rate alone results in changes in observed overall origination and extinction rates for the whole facies gradient.

An advantage of this model is its scale-independence and possible application to other influences on diversity such as geography or latitude. Additionally, preservation rates may be treated as relative amounts of total exposed rock representing each facies or as relative collection intensity among environments or regions.

We have used the model to explore the unusual decrease in origination rates characterizing the Late Devonian biotic crisis. The model predicts that a progressive decrease in preservation rate, rock amount, or collection intensity of nearshore facies (those with the highest taxonomic rates) produces a pattern of observed taxonomic rates remarkably similar to that seen in the Late Devonian, when origination rates decreased dramatically. Eustatic sea level changes and possible shelf anoxia in the Late Devonian may have affected nearshore facies more than offshore facies. True extinctions and ecological changes do occur during this interval. We do not suggest that preservation alone causes the observed Late Devonian diversity pattern, but that the trend may be influenced by rock record biases. One of the most important implications of this model result for the fossil record is that variable rates of preservation among facies may exert a strong control on overall observed taxonomic rates and diversity.

1D COMPACTION FLOW MODELING OF URSA CANYON

Louanne Christopher

Advisor: Peter Flemings

Masters Talk, Petroleum Theme

1-dimensional compaction forward modeling illustrates how overpressure may have developed in the Ursa Canyon basin due to rapid deposition of low permeability sediments above saturated sands. The Ursa Canyon basin is a known zone of overpressure, and a numerical model is used to illustrate how the overpressure condition of the sands in the Ursa basin are tied to porosity and permeability profiles, and initial conditions of deposition.

Compaction flow modeling focuses on how fluid behaves as sediments compact through gravity or increased loading. The flow model is tested by comparison with two analytical models, a diffusion solution by Turcotte and Schubert (2005) and the Gibson (1958) compaction model, before being populated with parameters to simulate the conditions at the Ursa Canyon. Simulated results are compared with a similar numerical model and observed pressure results from the International Ocean Drilling Program (IODP) Leg 308 Preliminary Drilling Report and found to underpredict the overpressure calculated from log-derived porosity data from Ursa.

AQUEOUS NUCLEATION AND GROWTH OF TITANIUM OXIDES USING TIME-RESOLVED SYNCHROTRON X-RAY DIFFRACTION

Daniel Hummer

Advisor: Peter Heaney

Pre-Comps Talk

The inorganic precipitation of oxide minerals in soil environments has profound effects on a variety of geochemical processes. These include the removal of metals from the aqueous phase, the production of coatings that reduce the reactive surface area of pre-existing mineral grains, and the generation of feedstocks for microbial metabolic reactions. Recent observations of transient, metastable phases during the growth of oxide crystallites has raised questions about their role in crystallization mechanisms, and created a need for more detailed structural measurements. To better understand the process of nucleation and growth, we investigated the crystallization of Ti oxides from aqueous 0.5 M TiCl_4 solutions using synchrotron X-ray diffraction at temperatures of 100 and 150 °C. Solutions were heated in a 1.0 mm internal diameter quartz glass capillary sealed with epoxy. Powder diffraction patterns of the growing crystallites were collected using image plate technology with a time step of ~ 4 minutes, providing high resolution *in situ* measurements of structural changes during the crystallization process.

The data indicate a co-precipitation of the two crystalline phases anatase and rutile within the first 30 minutes of heating, followed by a gradual phase transition from anatase to rutile during particle coarsening throughout the 10 hour duration of an experiment. The co-existence of anatase and rutile at the onset of crystallization lends additional support to the assertion of nearly identical free energies for anatase and rutile at the nanoscale, believed to be due to the prominence of surface energy effects (Ranade *et al.*, 2001). Whole pattern analyses using the Rietveld refinement method also documented previously unobserved changes in lattice parameters of both phases during growth, on the order of 0.2-0.3 % expansion for each axis. The trends in lattice parameters are observed to be temperature dependent, generally having lower values at higher crystallization temperature. In addition to increased surface energy, these small but measurable structural changes may be partially responsible for the observed reversals in thermodynamic stability between crystalline Ti oxide phases at very small particle sizes.

OXYGEN TOLERANCE IN 'STRICTLY' ANAEROBIC METHANOGENS

James Moran

Advisors: Katherine Freeman and Christopher House

Post-Comps Talk

Oxygen effectively poisons large groups of microorganisms and traditional paradigms hold that 'strict anaerobes' perish with oxygen exposure. Recent discovery of genes associated with oxygen detoxification in multiple anaerobic organisms challenge such a view and reveal potential mechanisms for oxygen resistance. Documented cases of anaerobes overcoming brief oxygen exposure suggest some anaerobes maintain mechanisms for resisting this extreme environmental condition, indicating the need for understanding both the distribution and extent of oxygen tolerance among prokaryotes.

We observed growth of multiple anaerobic Archaea and Bacteria cultures under varying microaerophilic conditions and are exploring their relative oxygen tolerance. Methanogenesis and biomass production (> 6 doublings) were observed in cultures containing a small partial pressure (~ 1 %) of oxygen in the headspace. We evaluated oxygen resistance in three methanogen species (*Methanosarcina acetivorans*, *Methanobacterium thermoautotrophicum*, and *Methanococcus maripaludis*), a sulfate reducer (*Desulfovibrio gigas*), and an acetogen (*Acetobacterium woodii*). We also evaluated a methanogen enrichment (*Methanohalophilus* sp.) for its relative oxygen tolerance. This enrichment originated from a hypersaline mat with unique juxtaposition of oxygen and anaerobic metabolism (namely methanogenesis and sulfate reduction) making it a prime candidate for studies of oxygen resistance.

Methanogenesis likely evolved early in Earth's history when its chemoautotrophic substrate requirements could be met in environments lacking complex organic matter. Since their evolution the Earth's biosphere has undergone extreme chemical alteration and yet methanogens persist in the modern world. Better understanding the lethal oxygen threshold for methanogens and other anaerobic species may help define their habitably regions in modern environments as well as help constrain the extent of these organisms through the changing environments of the past.

BASALT WEATHERING RATES ACROSS SCALES

Alexis Navarre

Advisor: Susan Brantley

Pre-Comps Talk

Weathering of silicate minerals is a known sink for atmospheric CO₂. An estimated 11.7×10^{12} mols of CO₂ are consumed each year by the weathering of silicates (Gaillardet *et al.*, 1999) and of that amount basalt weathering consumes 4.08×10^{12} mol/year of CO₂ (DESSERT *et al.*, 2003): therefore, 30%-35% of the consumption of CO₂ from continental silicate weathering can be attributed to basalt weathering. The aim of this paper is to compare basalt weathering rates across spatial and temporal scales to determine the best estimate of basalt weathering rates on Earth. To assess basalt weathering rates we examine rates of basalt alteration (L/t) reported at four scales: denudation rates from basalt watersheds (tens of kilometers), rates of soil formation from soil profiles developed on basaltic parent material of known age (meters), rates of weathering rind formation on basalt clasts (centimeters), and laboratory dissolution rates (millimeters). The effects of temperature, erosion and scaling on weathering rates have been examined.

Basalt weathering advance rates calculated for watersheds range between 0.36 and 9.8×10^{-3} mm/yr. Denudation rates for the Hawaii basalt soil profile is 8.0×10^{-3} mm/yr. Advance rates for weathering rinds are one to two orders of magnitude slower than the watershed and soil rates, ranging between 2.4×10^{-4} and 5.6×10^{-6} mm/yr. Batch and mixed flow laboratory experiment performed at circum-neutral pH yield advance rates of 2.5×10^{-5} to 3.4×10^{-7} mm/yr when normalized to BET surface area. These results show increasing advance rates with both increasing scale (from laboratory to watersheds) and increasing temperature. Activation energies for each of the scales are similar and range between 49 and 61 kJ/mol. Results from this study represent the first attempt to reconcile basalt weathering rates from laboratory, clast, soil profile, and watershed scales.

ARE WE DRUGGING OUR DRINKING WATER? OCCURRENCE, FATE AND TRANSPORT OF PHARMACEUTICALS AT PENN STATE'S LIVING FILTER

Jennifer Nemitz

Advisor: Richard Parizek

Pre-Comps Talk

Municipal wastewater treatment, remediation and recycling have become critical topics in the present eco-friendly age. The possible presence of pharmaceuticals and personal care products (PPCPs) in the water supply has been a hot topic since a sweeping study of US streams by the United State Geological Survey in 2002 found PPCPs in many of nation's streams. While the effect of these environmentally occurring PPCPs is largely unknown in humans, effects in aquatic populations include microbial resistance to antibiotics and the disruption of normal hormone function by endocrine disrupters. Endocrine disruption can influence aquatic populations even at very low concentrations, with the most visible sign being the feminization of fish, amphibians, and reptiles. The most common pathway PPCPs enter the environment is through the sewage system. Pharmaceuticals may not be fully metabolized within the human body and are released into the sewage treatment system through excrement. Once in the environment, pharmaceuticals generally occur in the aqueous phase and can rapidly degrade in the soil or environments with organic matter. However, constant loading from sewage discharge and other sources can have the same effect on organisms as if the pharmaceutical did not degrade.

Penn State's Living Filter is system in which secondary sewage effluent is sprayed onto cropland and forest land for remediation. Physical, chemical, and biological processes further treat the effluent, which then infiltrates through the soil column into the groundwater and is pumped back out as potable drinking water. The Living Filter has been in full operation for 20 years and the equivalent of a 200 foot deep lake has been filtered through its soils. The continued effluent loading at the Living Filter provides an excellent opportunity to detect the occurrence, fate and transport of PPCPs. Multiple hydrological environments including wetlands, overland flow, soil water, and groundwater allow for a complete systems approach to the fate and transport of PPCPs through the hydrologic cycle.

One liter composite effluent, surface water, soil water, groundwater, and wetland samples were collected, filtered through Empore disks, eluted, concentrated via Rotoevaporation, and analyzed using a GC/MS. Compounds detected included: 5-methyl-1H-benzotriazole, acetaminophen, caffeine, DEET, 2,6-di-tert-butylphenol, bis-(2-ethylhexyl) phthalate, estradiol, 17-alpha-ethinylestrodial, and cholesterol. A general scan mode was also used to try to identify other PPCPs outside of our selected PPCPs of interest. Four compounds appeared frequently: Dibutyl phthalate (a component of nail polish and hair spray), diethyl phthalate (a plasticizer), oleic acid (a component of hair color), and isopropyl palmitate (a component of hand cream, shampoo, and antiperspirant). Isopropyl palmitate was the most frequently occurring compound and was found in a total of 18 out of 47 water samples.

BASAL CONDITIONS NEAR THE ONSET OF ICE STREAM D, WEST ANTARCTICA

Leo Peters

Advisor: Sridhar Anandakrishnan

Pre-Comps Talk, Petroleum Theme

I present the results of a seismic reflection experiment performed near the onset of Ice Stream D, West Antarctica, that highlight lateral variations in basal conditions as ice flow shifts from slow internal deformation to ice streaming. By applying the amplitude variation with offset (AVO) technique to the ice-bed seismic reflection, I am able to constrain the seismic properties of the bed and better characterize the subglacial regime near this onset region. This technique reveals lateral variations in the geologic character of the bed, ranging from a soft, wet till, whose presence and continuity enhances ice flow, to drier, consolidated sediments that act as “sticky spots” at the bed of the ice stream. This spatial variability in basal conditions near the onset of Ice Stream D suggests that inland migration of streaming ice flow into the interior of West Antarctica is unlikely.

ORAL PRESENTATION SCHEDULE - WEDNESDAY MORNING

<u>Time</u>	<u>Presenter</u>	<u>Advisor</u>	<u>Title</u>
9:00	Tim Fischer	Peter Heaney	STABLE ISOTOPE COMPOSITION OF SPELEOTHEM CALCITE AND ASSOCIATED CAVE AND SOIL CO ₂ , CAVE OF THE BELLS, ARIZONA
9:15	Nathan Harkins	Eric Kirby	A COMPLEX RECORD OF FLUVIAL INCISION IN NE TIBET: IMPLICATIONS FOR LANDSCAPE RESPONSE TO TECTONICS
9:30	Audrey Hucks	Peter Flemings	HYDROLOGIC MONITORING IN THE NANKAI ACCRETIONARY PRISM
9:45	Christina Lopano	Peter Heaney	EXCHANGE RATES IN SYNTHETIC BIRNESSITE MEASURED BY TIME-RESOLVED SYNCHROTRON X-RAY DIFFRACTION
10:00	BREAK		
10:15	Heather Savage	Susan Brantley	THE POTENTIAL FOR EARTHQUAKE TRIGGERING BY TRANSIENT DEFORMATION
10:30	Irene Schneider	James Kasting	CHARACTERIZATION OF THE RADIATION ON THE SURFACE OF MARS AND ITS ASTROBIOLOGICAL IMPLICATIONS
10:45	Elisabeth Hausrath	Susan Brantley	REACTIVE TRANSPORT MODELING OF BASALT WEATHERING UNDER MARS-LIKE CONDITIONS

STABLE ISOTOPE COMPOSITION OF SPELEOTHEM CALCITE AND ASSOCIATED CAVE AND SOIL CO₂, CAVE OF THE BELLS, ARIZONA

Tim Fischer

Advisor: Peter Heaney

Pre-Comps Talk

The $\delta^{13}\text{C}$ value of cave speleothem calcite can be interpreted in various ways. A popular method is to interpret these values using a soil diffusion model and connect the $\delta^{13}\text{C}$ values to paleovegetation in the form of proportion of C₃ to C₄ biomass living in the soil above the cave. A potential problem with these interpretations is the uncertainty as to the validity of the use of this model. Here we present $\delta^{13}\text{C}$ measurements of plants, soil carbonate, soil organic matter, cave-air CO₂, soil-respired CO₂ and soil CO₂ in an effort to establish the validity of the soil diffusion model for the Cave of the Bells in Southeastern Arizona. We found that the predicted value of “modern” speleothem calcite based on our average cave-air CO₂ $\delta^{13}\text{C}$ of -19‰ to be approximately 1.5‰ lower than actual “modern” speleothem values. This indicates that CO₂ diffusion is not the only mechanism involved in the fixing of the $\delta^{13}\text{C}$ value. Soil organic matter taken from the vicinity of the cave matches the cave-air CO₂ $\delta^{13}\text{C}$, which implies that no CO₂ diffusion is taking place within the cave. However, since pCO₂ is high in the cave throughout the course of a year (7000-12000 ppmV), it is possible that production of CO₂ is so much greater than diffusive loss that CO₂ entering the cave from the soil drowns out any other signal. This study represents the first attempt to combine the $\delta^{13}\text{C}$ values from various substrates in a cave system and will hopefully be used as a starting point and an example for the future interpretation of cave speleothem $\delta^{13}\text{C}$ values.

A COMPLEX RECORD OF FLUVIAL INCISION IN NE TIBET: IMPLICATIONS FOR LANDSCAPE RESPONSE TO TECTONICS

Nathan Harkins

Advisor: Eric Kirby

Pre-Comps Talk

Many tectonic geomorphic analyses necessarily assume a condition of topographic steady state (where erosion balances rock uplift and topography is temporally invariant) in order to interpret tectonic signals from landscape topography [e.g., *Adams, 1985; Willgoose et al., 1991; Simoni et al. 2005*]. The rate of change associated with various landscape forcing mechanisms (climate, land cover, tectonism, etc.), however, are potentially shorter than the total duration of landscape adjustment to those mechanisms [e.g., *Whipple and Tucker, 1999; Whipple, 2001*]. As a result, most landscapes likely host a transient form that preserves a richer record of both an older, and a more recent set of forcing mechanisms than previously considered. The upstream migration of channel knickpoints has been suggested to be the primary means of transient fluvial adjustment to a change in forcing mechanisms. Much progress has been made towards understanding the genesis and propagation of fluvial knickpoints along single channel systems. Little is known, however, about the timescales and kinematics associated with the migration of a knickpoint through a 'real-world' setting of complex fluvial networks and spatially variable rock uplift rates. We investigate a distinct transient wave of incision observed in the tributaries and main channel of the Yellow River NE Tibet. Fluvial incision rates within this wave are measured from dated terrace surfaces at 1.3-1.8 mm/yr since the late Pleistocene. Obvious knickpoints in channels mark the upstream limit of this transient wave. Observed knickpoints display an invariant vertical propagation rate despite differences in host channel size, a behavior predicted by a simple geometric derivation of knickpoint propagation speed. Channel gradients and incision rates upstream of knickpoints, with measured rates < 0.5 mm/yr, preserve a record of the much slower, near steady-state incision rates prior to the wave. Comparison of measured incision and basin exhumation rates to channel k_s values (channel gradients normalized to a reference concavity) yields an apparent, near-linear relationship between the two. This relationship is used to delineate increased fluvial incision rates that are adjusted to, and identify a broad zone (~200 km wide) of heightened rock uplift rates that straddles the eastern terminus of the Kunlun fault. The description of a broad uplift around this major continental strike-slip fault zone has important implications for the large-scale mechanics and crustal rheology of the Tibetan Plateau. Additionally, recognition of this incisional wave along the Yellow River helps to define an apparent, progressive, and ongoing evacuation of terrestrial basins that is dramatically changing the NE Tibetan plateau topography.

REACTIVE TRANSPORT MODELING OF BASALT WEATHERING UNDER MARS-LIKE CONDITIONS

Elisabeth Hausrath

Advisor: Susan Brantley

Pre-Comps Talk

Despite the extensive evidence for water on Mars, it is not clear how long water may have been present as a liquid. The duration and characteristics of liquid water on Mars strongly affect the possibility for the evolution of life. Observations of weathering products and the stability or instability of primary minerals on Mars may provide some constraints on the presence of liquid water. For example, relatively unaltered olivine, phyllosilicates, and sulfates have all been observed to be present on the surface of Mars. Rates of dissolution of olivine and other primary minerals, and the formation of phyllosilicates and other secondary minerals may help constrain the duration and characteristics of water on Mars.

We are characterizing basalt weathering in a Mars Analogue Site, Sverrefjell in Svalbard, Norway. Sverrefjell is considered an excellent analogue for water-rock interactions on Mars because of the cold and dry weather conditions and the similarity in rock type. We are modeling the basalt weathering observed in Svalbard using the reactive transport code CrunchFlow so as to account for both transport and reaction processes and to interpret spatial patterns on the Martian surface. The use of CrunchFlow to model basalt weathering under conditions relevant to Mars may help us better constrain the duration and characteristics of water on Mars.

HYDROLOGIC MONITORING IN THE NANKAI ACCRETIONARY PRISM

Audrey Hucks

Advisor: Peter Flemings

Pre-Comps Talk, Petroleum Theme

Measured pressure responses to tidal loading and deformation-induced strain events vary significantly in amplitude and timing among monitoring depths within a single ACORK. Tidal pressure responses are extremely diminished (to less than 10% of seafloor amplitudes) at several monitoring screens in the Lower Shikoku Basin facies, a low-permeability hemipelagic unit. The tidal pressure responses at these screens also display large lags or leads (~ -330 or +30 degrees). The low permeability of the Lower Shikoku Basin facies alone cannot account for the attenuated, and phase shifted, tidal pressure responses. We present a model for ACORK response to sinusoidal formation pressure changes and show that to reproduce observed amplitudes, the system compliance must be at least 100 times greater than that predicted by a simple mechanical calculation. The compliant ACORK behavior may be due to skin effects (a zone of altered permeability around the borehole created during drilling) or free gas in the instrument. We favor the skin effect due to its large impact on tidal pressure response: a centimeter-thick drilling disturbance zone with a permeability 100 times lower than the surrounding undisturbed formation can alter amplitude by up to 70% and phase by over 1000%. Conducting slug tests at multiple ACORK screens during the next data recovery cruise would make full characterization of permeability, skin, and instrument compliance possible.

KINETIC ANALYSES OF CATION EXCHANGE RATES IN SYNTHETIC BIRNESSITE MEASURED BY TIME-RESOLVED SYNCHROTRON X-RAY DIFFRACTION

Christina Lopano
Advisor: Peter Heaney
Post-Comps Talk

Birnessite is the most abundant and chemically important layer-structure Mn-oxide phase found in soils, desert varnishes, and ocean nodules. It also is industrially important for use in battery technology and octahedral sieves. Due to the poorly crystalline nature of natural birnessite, synthetic analogues typically have been employed in studies that explore the structural response of birnessite to variations in interlayer composition. For this work, we measured changes in unit-cell parameters over time to quantify the degree of cation exchange as a function of concentration. Aqueous K^+ , Cs^+ , and Ba^{2+} cations at varying concentrations at pH 7 were exchanged for interlayer Na^+ in synthetic birnessite ($Na_{0.58}(Mn^{4+}_{1.42}, Mn^{3+}_{0.58})O_4 \cdot 1.5H_2O$) using a simple flow-through cell, and the exchange products were monitored via time-resolved X-ray powder diffraction at the National Synchrotron Light Source. Powder X-ray diffraction patterns were collected every 2-3 minutes.

Rietveld analyses of X-ray diffraction patterns for K- and Ba-exchanged birnessite revealed a decrease in unit-cell volume over time. In contrast, Cs^+ substitution increased cell volume. For all three cations, the crystallographic data indicate that exchange occurred in two stages. A rapid and dramatic change in unit-cell volume was followed by a modest adjustment over longer timescales. Fourier electron difference syntheses revealed that the rapid, initial stage of exchange was marked by re-configuration of the interlayer species, whereas the second, protracted phase of substitution represented ordering into the newly established interlayer positions.

For the first time, we have modeled the kinetics of interlayer substitution in Na-birnessite. For purposes of comparison, we have employed a simple one-stage reaction (i.e., Na-birnessite \rightarrow K-birnessite) and a two stage reaction (i.e., Na-birnessite \rightarrow K-birnessite_(disordered) \rightarrow K-birnessite_(ordered)). For exchange with 0.01 M KCl solutions, the single-stage model produced the following rate equation: $R = 0.081 \cdot X_{Na} \cdot [K_{(aq)}]$. The two-stage model generated a rate equation of $R = 0.146 \cdot (1 - (X_{K(dis)} + X_{K(ord)})) - 0.01153 \cdot X_{K(dis)}$. In both reactions, $[K_{(aq)}]$ is the molar concentration of the aqueous cation, X is mole fraction interlayer cation, and R is the rate of exchange in terms sec^{-1} . We assume a linear relationship between mole fraction and unit-cell volume based on Vegard's Law. Further kinetic analyses are in progress in order to determine the cation exchange rate dependence on concentration and to compare cation exchange rates for K-, Cs- and Ba-exchange.

THE POTENTIAL FOR EARTHQUAKE TRIGGERING BY TRANSIENT DEFORMATION

Heather Savage

Advisor: Chris Marone

Post-Comps Talk

Remote triggering of earthquakes is the promotion of fault failure by deformations associated with passing seismic waves. However, not all large earthquakes trigger remote seismicity. Debate exists over what characteristics of the seismic waves are important and thus, what mechanisms control failure. We propose that in addition to seismic wave characteristics, fault zone architecture will modify the effects of triggering mechanisms. The creation of gouge within a fault zone can cause faults that are slipping unstably to commence stable sliding. We find that gouge layers will also decrease triggered seismicity on a locked fault.

Experiments were conducted on laboratory faults using a servo-controlled biaxial deformation apparatus. Different fault architectures were replicated by using both thick and thin layers of synthetic gouge material, as well as bare granite surfaces. We analyze the dependence of dynamic triggering due to characteristics of the triggering event such as amplitude and frequency of the seismic wave as well fault state, i.e. the time since the last earthquake on that fault. The seismic waves from a triggering earthquake and tectonic loading were simulated by superimposing a transient shear load sinusoid on a constant shear load. Faults experiencing constant load fail with a consistent recurrence interval. We compare these to the recurrence times for faults under transient load conditions and infer shortening of recurrence interval as earthquake triggering.

Seismic wave amplitude affects triggering in all fault settings, however bare surfaces are the most susceptible to triggering. Although a thin gouge layer weakens fault shear strength, larger amplitude waves are required for triggering to occur. The faults with the thickest gouge layers display the least propensity for transient triggering. The frequency dependence of transient triggering presents a more complicated story. High frequency oscillations more easily trigger failure on faults with thick gouge layers than faults with thin gouge layers. Faults without gouge zones show no frequency dependence. These results imply that failure is most easily achieved on faults without gouge zones, which tend to be shorter in length and have less displacement. However, when seismic waves are large enough to trigger seismicity on faults with well-developed gouge zones, the frequency content of the seismic wave will affect triggering.

CHARACTERIZATION OF THE RADIATION ON THE SURFACE OF MARS AND ITS ASTROBIOLOGICAL IMPLICATIONS

Irene Schneider

Advisor: James Kasting

Masters Talk

Little is known about the radiation environment on the surface of Mars due to the fact that no lander/probe has ever carried nuclear radiation detection equipment to characterize it. The first mission set to precisely accomplish this task, the Mars Science Laboratory or MSL, is not due to launch until 2006. In this manner, only the incoming cosmic radiation and the solar particle events had been considered, while the scattered nuclear radiation contribution was usually neglected or ignored.

However, the recent detection of subsurface hydrogen on Mars, has prompted an in depth study of this backscattered contribution. In addition to this, recent simulations utilizing specialized nuclear transport codes have produced results which indicate that this contribution might in fact be quite significant and thus it must be accounted for.

Presented here are some preliminary estimates for these nuclear radiation doses as delivered by thermal, epithermal and fast neutrons which are arising from nuclear interactions of the incident cosmic rays with first the Martian atmosphere and second with the Martian regolith. Finally, a view of the Astrobiological implications is given in view of terrestrial planet habitability.

ORAL PRESENTATION SCHEDULE - WEDNESDAY AFTERNOON

<u>Time</u>	<u>Presenter</u>	<u>Advisor</u>	<u>Title</u>
1:00	James Fulton	Michael Arthur, Katherine Freeman	EVOLUTION OF PRIMARY PRODUCTION IN A MERMICTIC LAKE AND IMPLICATIONS FOR SEDIMENTARY $\delta^{15}\text{N}$ INTERPRETATIONS
1:15	Gavin Hayes	Kevin Furlong	EVIDENCE FOR MELT INJECTION IN THE CRUST OF CALIFORNIA?
1:30	Courtney Johnson	Kevin Furlong	POTENTIAL EARTHQUAKE HAZARDS ASSOCIATED WITH PREVIOUSLY UNRECOGNIZED BLIND THRUST FAULT: ANALYSIS OF THE MARIN COUNTY – MT. TAMALPAIS REGION
1:45	Christopher Junium	Michael Arthur	DIVERSITY AND VARIABILITY OF GEOPORPHYRINS AND CHLORINS DURING CRETACEOUS OCEANIC ANOXIC EVENT II
2:00	BREAK		
2:15	Derek Sawyer	Peter Flemings	PHYSICAL PROPERTIES OF MASS TRANSPORT DEPOSITS: IMPACT ON OFFSHORE HYDROCARBON EXPLORATION AND DEVELOPMENT
2:30	Robert Selover	Rudy Slingerland	OCEAN CIRCULATION AND SEDIMENT TRANSPORT PATS IN THE GULF OF PAPUA
2:45	Jennifer Williams	Susan Brantley	PROPOSAL FOR EXTRACTION OF WEATHERING RATES FROM MODERN SOIL PROFILES
3:00	Yongcheol Park	Andrew Nyblade	UPPER MANTLE STRUCTURE BENEATH THE ARABIAN PENINSULA FROM BODY AND SURFACE WAVE TOMOGRAPHY

EVOLUTION OF PRIMARY PRODUCTION IN A MEROMICTIC LAKE AND IMPLICATIONS FOR SEDIMENTARY $\delta^{15}\text{N}$ INTERPRETATIONS

James Fulton

Advisors: Michael Arthur and Katherine Freeman

Pre-Comps Talk

Fayetteville Green Lake, located near Syracuse, NY, has contained anoxic bottom water below a chemocline for most of the Holocene Epoch, resulting in excellent preservation of organic matter in its laminated sediments. Similar conditions are found in the modern Black Sea and have existed in ocean basins in the past, resulting in organic-matter-rich black shales. Methods for interpreting $\delta^{15}\text{N}$ of sedimentary organic matter in sapropels and black shales typically assume that $\delta^{15}\text{N}$ values below 0‰ result from nitrogen fixation by diazotrophic cyanobacteria or green sulfur bacteria. This work examines the relative roles of phototrophs above and below the chemocline in the total productivity of the lake, and how variability in this balance ultimately effects changes in $\delta^{15}\text{N}$ expressed in the sediments.

Previous studies suggest that deforestation of Green Lake's drainage basin in the early 19th century stimulated higher rates of organic matter production in the lake due to increased nutrient flux. Primary productivity increased both below and above the chemocline, shown by increased accumulation rates of bulk organic matter as well as Chl *a*, Bchl *a*, and Bchl *e*. However, the waters above the chemocline experienced a greater increase in productivity, expressed in part by the ratios of Chl *a*:Bchl *a* and Chl *a*:Bchl *e* in the sediments. I have also found that prior to the nutrient increase anoxygenic green and purple sulfur bacteria ($\delta^{13}\text{C} = -31\text{‰}$ to -42‰) composed a significant fraction of preserved sedimentary organic matter ($\delta^{13}\text{C} = -32\text{‰}$). The higher nutrient influx increased plant and algal productivity above the chemocline, thereby enriching sedimentary $\delta^{13}\text{C}$ values (-24‰ to -28‰). Relatively enriched $\delta^{15}\text{N}$ values (ca. 3.7‰) in sediments deposited during the past ~200 years also reflect increased production in the surface mixed layer. Prior to the increase in nutrient flux, sedimentary $\delta^{15}\text{N}$ ranged between 1.5‰ and 2.5‰, reflecting biological fractionation during uptake of ammonium from below the chemocline. Modern $\delta^{15}\text{N}$ values for suspended particulate matter at the chemocline are below 0‰ and ammonium $\delta^{15}\text{N}$ is 14-17‰. The results from this study illustrate a mechanism for relative ^{15}N -depletion in sediments that does not require nitrogen fixation, as ^{15}N -depletion also may result from a large pool of ammonium supporting growth of anoxygenic bacteria preferentially assimilating $^{14}\text{NH}_4^+$.

EVIDENCE FOR MELT INJECTION IN THE CRUST OF CALIFORNIA?

Gavin Hayes

Advisor: Kevin Furlong

Pre-Comps Talk

The position of Cenozoic volcanism in the crust of the northern California Coast Ranges is directly linked to the northward migration of the Mendocino triple junction (MTJ) and the formation of a slab window beneath North American crust. The most recent manifestation of this is the Clear Lake volcanics, which began erupting ~2Ma. With the continued migration of the triple junction, volcanic activity is expected further north of Clear Lake in the future. These volcanic centers erupt in areas where the crust is undergoing significant modification as a result of slab window processes, and reflect important components in the development of the San Andreas plate boundary system. The occurrence of an earthquake sequence near Lake Pillsbury, California during a six-month period in mid-2000 can be linked to magma transport in the crust; this activity is potentially a pre-cursor to future volcanism. When precisely relocated, the earthquake sequence defines a streak of seismicity at ~8km depth. This sequence demonstrates a local time-space migration over a distance of ~10km in two major pulses of activity in the 6-month time period. Stress modeling allows us to infer that these earthquakes may be the result of several dike injections. In combination with evidence for lower crustal melts in the same region from other seismological studies, we propose that these earthquakes help map the occurrence of melt injection in the mid-crust to depths of ~10km, and present evidence that MTJ-related melt in the crust of northern California has migrated north of the Clear Lake volcanic center.

POTENTIAL EARTHQUAKE HAZARDS ASSOCIATED WITH PREVIOUSLY UNRECOGNIZED BLIND THRUST FAULT: ANALYSIS OF THE MARIN COUNTY – MT. TAMALPAIS REGION

Courtney Johnson
Advisor: Kevin Furlong
Masters Talk

The major strike slip faults of the San Andreas fault system are the primary earthquake hazard in the San Francisco Bay area. Complex fault geometries and discrepancies in fault slip rates, however, imply that there may be additional structures such as blind thrusts in the region to transfer slip among the faults in the system. Blind thrusts have often remained unrecognized hazards within the San Andreas fault system until a damaging event occurs. Two recent examples are the 1994 Mw 6.7 Northridge and 2003 Mw 6.5 San Simeon events. We propose that a blind thrust beneath the Mt. Tamalpais and Marin County region, just north of San Francisco, is an active structure that solves a slip rate discrepancy and has produced the enigmatic elevations in the area, and can potentially host moderate earthquakes. We have combined geomorphic analyses of stream channels and the landscape in the Marin County – Mt. Tamalpais region with seismicity, fault behavior, and deformational modeling to assess the potential hazard from this proposed structure.

Geomorphic analyses of stream channels within the elevated region show a systematic change in channel steepness with location. Exploiting relationships between channel steepness and uplift rate, we can constrain models of blind thrust deformation that can produce the modern landscape, when erosion is included. This study, coupling deformational modeling with geomorphic constraints on erosion to analyze the potential for a blind thrust beneath Mt. Tamalpais, allows us to place important constraints on rates and extent of fault slip.

From this integrated analysis of geophysical, geomorphic, geochronologic, geodetic and geodynamic observations, we are able to estimate that a simple blind thrust capable of producing Mt. Tamalpais could host a Mw = ~6.8 with recurrence of ~300 years. Such a fault poses an additional earthquake hazard beneath Mt. Tamalpais and Marin County, with the potential for the majority of ground shaking to occur up-dip of the structure, towards San Francisco.

DIVERSITY AND VARIABILITY OF GEOPORPHYRINS AND CHLORINS DURING CRETACEOUS OCEANIC ANOXIC EVENT II

Christopher Junium
Advisor: Michael Arthur
Pre-Comps Talk

Geoporphyrins and chlorins are biomarkers that result from the transformation of tetrapyrroles including chlorophylls, bacteriochlorophylls and haems. The transformation reactions are initiated in the water column and sediments during early diagenesis and are dependent on a range of variables including, but not limited to water column redox state, burial conditions, and time. Geoporphyrins and chlorins can retain structural characteristics that allow unambiguous assignment of precursor structures and source organisms making their utility in paleoenvironmental studies extraordinary where such information is preserved. Black shales from Oceanic Anoxic Event II (OAE II, Cenomanian-Turonian Boundary) of ODP Leg 207 present a unique opportunity for investigating the variations in the tetrapyrrole record in very well preserved sediments across a globally significant biogeochemical event. Identification and structural assignment of tetrapyrroles in this study were achieved by a combination of high-performance-liquid-chromatography (HPLC)/diode-array-detection (DAD) and liquid chromatography-mass spectrometry (LC-MSⁿ) on acetone extracts.

Stratigraphic variations in geoporphyrin compounds occur through OAE II. The relative proportions of metallated vs. free-base (metal free) porphyrins vary throughout the sequence, favoring free-base porphyrins during the height of the anoxic event. The greater proportion of free-base porphyrins associated with more extensive reducing conditions is consistent with metal ion limitation during euxinia. For example, vanadyl porphyrins become much less abundant during the peak of the event suggesting that the oceanic inventory of V was sequestered in black shales and unavailable.

Preliminary characterization of the tetrapyrroles through OAE II of ODP Leg 207, Demerara Rise, reveals a wide range of geoporphyrins and chlorins. Notably, positive identification of chlorins, the geologically unstable intermediates between highly reactive chlorophylls and the more stable geoporphyrins, predates the previous oldest described sedimentary occurrence by more than 70 Ma (Miocene, Vena del Gesso). Presence of chlorins implies exceptional preservation associated with strongly reducing conditions that existed during OAE II at Demerara Rise and the excellent condition of the recovered core material. Chlorins attributed to green sulfur bacteria, on the basis of specific mass-spectral characteristics 43 and 57, confirm the presence of anaerobic photoautotrophs and periods of photic-zone euxinia at Demerara Rise during the mid-Cretaceous. Unusually high abundances of the C33 bicyclo-alkanoporphyrin were also observed. The C-33 bicyclo-alkanoporphyrin is possibly derived from rearrangement of chlorophyll a and suggests that a high proportion of the extractable geoporphyrins were derived from cyanobacteria and calcareous nannoplankton.

PHYSICAL PROPERTIES OF MASS TRANSPORT DEPOSITS: IMPACT ON OFFSHORE HYDROCARBON EXPLORATION AND DEVELOPMENT

Derek Sawyer

Advisor: Peter Flemings

Masters Talk, Petroleum Theme

Shear strength, bulk density, resistivity logs, and the degree of sediment deformation vary significantly within a mass transport deposit (MTD) along a ~10 km transect as documented from IODP Expedition 308 Sites U1324 and U1322 in the northern Gulf of Mexico. We demonstrate that the deposits of slumps and slides have physical properties much like normally deposited sediment whereas debris flow deposits have a significantly more compacted nature. MTDs are the products of large submarine landslides and contain a range of deposits from relatively simple slides and slumps to more disintegrative debris flows. Because of the tendency to be more compacted, they are recognized as a potential hazard in the hydrocarbon industry. They can dramatically slow the penetration rate of jet pipes, and suction anchor piles, which form the foundation to many exploration and development sites. The MTD of focus in this study was deposited ~20 kya, lies ~100 meters below the seafloor, is ~40-100 meters thick, is composed of mud, and covers an area of ~1000 km² in the Mars-Ursa oilfield region 200 km southeast of New Orleans, Louisiana. It is easily recognized in high-resolution 3-D and conventional exploration 3-D seismic data by a sharp, stepped basal detachment surface, and internal chaotic to semi-transparent seismic facies. The bulk physical properties of the MTD show significant variations, despite having similar internal seismic facies at both sites. At Site U1322, lower porosity, higher shear strength, higher core deformation, and higher logging resistivity distinguish the MTD relative to the surrounding unfailed sediments. However, 10 km to the west-southwest at Site U1324, no significant offsets are observed in shear strength, porosity, or LWD resistivity, and only minor core deformation is observed. Seismic attributes such as interval amplitude extractions generally correspond to this variation in the bulk physical properties. Interval amplitude extractions of the MTD reveal sinuous flow pathways in the area of Site U1322. However, no such features are observed around Site U1324. We interpret that debris flows (disintegrative failure and relatively long runout distance) developed in the area of Site U1322, while only slumps slides (minor strain and relatively short runout distance) formed in the area of Site U1324. Our work demonstrates that the physical properties within an MTD can depend on the specific process that created it (slumps vs. debris flows). Our work is applicable to geohazards assessments that are required for offshore wells and subsea installments, and illuminates the underlying processes and products associated with MTDs.

OCEAN CIRCULATION AND SEDIMENT TRANSPORT PATH IN THE GULF OF PAPUA

Robert Selover

Advisor: Rudy Slingerland

Masters Talk

To develop a model for clinoform genesis in the Gulf of Papua (GoP) we have simulated regional circulation during 2003 using the Navy Coastal Ocean Model (NCOM) at 0.03° horizontal resolution. The model is nested within the East Asian Seas implementation of NCOM which assimilates monthly mean discharges for 51 rivers, synthetic temperature and salinity profiles, and altimetry. Surface boundary conditions consist of heat fluxes, precipitation, surface pressure, and wind stresses from an operational weather model (Navy Operational Global Atmospheric Prediction System). Results show two general circulation states highly influenced by seasonal monsoon/trade winds. During the northwest monsoon the surface circulation consists of an alternation between CW ($\sim 0.1\text{-}0.2$ m/s NE) and CCW (~ 0.04 m/s SW) gyres which match the oscillatory wind patterns during this period. This alternation creates zones of downwelling (mean flux $\sim 0.08\text{E-}2\text{Sv}$) along the modern clinoform face. During early March 2003, severe Tropical Cyclone Erica (max wind speed $\sim 185\text{km/hr}$) crossed the GoP resulting in a sustained CW gyre with mean flows of $\sim 0.15\text{m/s}$ NE. The trade wind season is marked by an end to the oscillating gyre circulation pattern and a transition to an intense NE-directed flow along the clinoform face (mean flow $\sim 0.35\text{m/s}$ at surface; $\sim 0.05\text{m/s}$ at depth). On the shelf near the Fly River, surface currents vary from westward to southwestward with speeds of $0.1\text{-}0.2$ m/s. Bottom currents of less than 0.1 m/s during the trade-wind season are generally to the southwest. Along the north coast the surface flow is weaker and fluctuates as the wind changes direction. The surface flow near the northeast coast is uniformly southeast with currents as high as 1 m/s. These results suggest a sediment dispersal pattern consisting of SW transport on the modern clinoform topset, and NE transport on the fore- and bottom-sets.

PROPOSAL FOR EXTRACTION OF WEATHERING RATES FROM MODERN SOIL PROFILES

Jennifer Williams
Advisor: Susan Brantley
Pre-Comps Talk

Evolution of the Earth's surface is of great interest to geochemists as it provides insights into mechanisms, which have propagated through history. Although many scientists would argue the extent to which we understand climatic influences on the cycling of elements that are essential for all life, new disciplines are developing in order to integrate biology and microbiology with geochemistry and kinetics to answer more complex questions. In this regard, studying climosequences which cover temperature and precipitation gradients should shed light on some of these multifaceted processes. Specifically, one representative climosequence is the Mississippi River Valley, where various researchers have studied the soil developed on Peoria Loess. Radiocarbon dating marks deposition of the Loess occurred from 23,000 – 10,000 years, with modern soil pedogenesis slated to have begun between 13,000 and 10,000 years. Historic data suggests the past vegetation and climate was mesic deciduous forest.

Sampling of twenty two pedons for analysis, using x-ray fluorescence, occurred from Iowa to Louisiana. Most samples were collected from well-drained, but uneroded upland localities, with the exception of five, which were collected from cultivated lands. In this particular region, the complexity of soils creates an interesting opportunity to determine solid-state fluxes within pedons derived essentially from the same parent material. Using these fluxes, a comparison of elemental loss in relation to latitude may suggest a mechanism which propagates throughout the valley or is represented only locally.

UPPER MANTLE STRUCTURE BENEATH THE ARABIAN PENINSULA FROM BODY AND SURFACE WAVE TOMOGRAPHY

Yongcheol Park
Advisor: Andrew Nyblade
Post-Comps Talk

We have imaged tomographically the three-dimensional velocity structure of the upper mantle beneath the Arabian Peninsula using teleseismic P- and S-waves and Rayleigh wave phase velocities. The data came from the Saudi Arabian National Digital Seismic Network (SANDSN) operated by King Abdulaziz City for Science and Technology (KACST: 21 broadband stations and 4 short-period stations). We augmented the KACST data with delay times measured from permanent Incorporated Research Institutions for Seismology (IRIS) stations in the region (RAYN, EIL and MRNI) and the 1996 Saudi Arabian PASSCAL Experiment (9 broadband stations). The P- and S wave models were inverted from 401 earthquakes resulting in 3416 ray paths with P- and PKP-wave arrivals, and 1602 ray paths with S- and SKS-wave arrivals came from 201 earthquakes, respectively. The P and S wave models yield consistent results. The models show strong low velocity regions beneath the southeastern Arabian Shield and the mid-eastern edge of Arabian Shield. The low velocity anomaly in the southeastern part of the Arabian Shield does not extend north of 21°N and dips to south. It likely represents the northeastern edge of the Afar hotspot. Surface wave tomography is being performed using fundamental mode Rayleigh wave phase velocities measured across the SANDSN. Preliminary phase velocity maps will be provided and compared to the body wave tomographic results.

ORAL PRESENTATION SCHEDULE - THURSDAY MORNING

<u>Time</u>	<u>Presenter</u>	<u>Advisor</u>	<u>Title</u>
9:00	Aubrey Adams	Andrew Nyblade	LITHOSPHERIC STRENGTH OF ZAGROS MOUNTAINS IN IRAN: A JELLY-SANDWICH OR CRÈME BRÛLÉE?
9:15	Ellen Currano	Peter Wilf	INCREASED INSECT HERBIVORY DURING THE PALEOCENE-EOCENE THERMAL MAXIMUM IN THE BIGHORN BASIN, WYOMING USA
9:30	Doug Edmonds	Rudy Slingerland	MECHANICS OF MIDDLE-GROUND BAR FORMATION: IMPLICATIONS FOR THE MORPHODYNAMICS OF DELTA CHANNEL NETWORKS
9:45	Mouse Marie Larson	Andrew Nyblade	EXAMINING THE MANTLE TRANSITION ZONE BENEATH THE TRANSANTARCTIC MOUNTAINS FROM RECEIVER FUNCTIONS USING TAMSEIS
10:00	BREAK		
10:15	Katja Meyer	Lee Kump	QUANTITATIVE EVALUATION OF H ₂ S ERUPTIONS FROM THE END-PERMIAN OCEAN
10:30	Kristin Morell	Donald Fisher	FOREARC RESPONSE TO THE MIGRATING PANAMA TRIPLE JUNCTION
10:45	Aaron Regberg	Susan Brantley, Kamini Singha	CAN HYDROGEOPHYSICAL TOOLS BE USED TO IMAGE BIOGEOCHEMICAL REACTION RATES IN THE SUBSURFACE?
11:00	Jason Sitchler	Donald Fisher	DEFORMATION OF THE PANAMA MICROPLATE IN RESPONSE TO AN ABRUPT INCREASE IN PLATE BOUNDARY COUPLING

LITHOSPHERIC STRENGTH OF ZAGROS MOUNTAINS IN IRAN: A JELLY-SANDWICH OR CRÈME BRÛLÉE?

Aubrey Adams

Advisor: Andrew Nyblade

Pre-Comps Talk

The rheologic strength of lithospheric rocks comprising the crust and upper mantle beneath the Zagros Mountains of southwestern Iran is a subject of current debate. Some early studies claim that the lithosphere in this area follows the “jelly sandwich” model, having a weak, ductily deforming lower crust that lies between a strong upper crust and a strong upper mantle. More recent studies, however, have likened the structure of the Zagros Mountains’ lithosphere to crème brûlée, with a strong upper crust overlying a weak lower crust and a weak upper mantle. This study presents preliminary evidence for earthquake sources at depths throughout the crust. These results indicate that the entire crust beneath the Zagros Mountains is strong enough to support brittle deformation through earthquake rupture. Thus, the preliminary data presented here does not support either the “jelly sandwich” or the “crème brûlée” lithospheric models.

INCREASED INSECT HERBIVORY DURING THE PALEOCENE-EOCENE THERMAL MAXIMUM IN THE BIGHORN BASIN, WYOMING USA

Ellen Currano
Peter Wilf
Pre-Comps Talk

Climates, biodiversity, and organismic distributions changed significantly across the Paleocene-Eocene boundary. In Wyoming's Bighorn Basin, major temperature fluctuation was accompanied by strong turnover in plants and mammals. Although food webs incorporating plants and phytophagous insects account for up to 75% of global biodiversity, the responses of insect herbivores to climatic and floral change have not been well-studied. The research presented here is part of a larger project to examine changes in insect damage on angiosperm leaves in the Western Interior, USA, through the Paleocene and Eocene. Our objective is to test how changes in climate, resource limitations, and floral diversity affected the recovery of insect herbivores from the Cretaceous-Tertiary (K-T) extinction. We focus here on insect damage in the Bighorn Basin during the late Paleocene and early Eocene (59 – 55.8 Ma), with particular emphasis on the Paleocene-Eocene Thermal Maximum (PETM).

We conducted insect damage censuses at four sites in the Bighorn Basin in 2002 and 2005, informally named Skeleton Coast (Tiffanian 4, ~59.0 Ma), Lur'd Leaves (Tiffanian 5, ~57.5 Ma), Daiye Spa (Clarkforkian 3, ~56 Ma), and Hubble Bubble (PETM, 55.8 Ma). Additionally, an earliest Eocene flora is currently under study. The late Paleocene localities have relatively low floral diversities and span a gradual warming.¹ Hubble Bubble is stratigraphically in the middle of the PETM and has a significantly higher floral diversity than the other sites. At each locality, between 750 and 1350 identifiable dicot leaves were scored for insect damage using the damage morphotypes (DTs) of Labandeira *et al.*² These DTs can be divided into those typical of generalist insects and those strongly associated with oligophagous or monophagous specialist herbivores, such as mines and galls. Damage metrics were compared for the bulk floras using random resampling with replacement to standardize for sample size.

Insect herbivory increases through the late Paleocene and reaches a maximum in the PETM. Between 15 and 38% of angiosperm leaves from the three Paleocene localities contain insect damage, whereas 56% of the PETM leaves are damaged. When resampled at 750 leaves, Skeleton Coast has 18.7 total DTs, 7.8 specialized DTs, and 0.9 mine types. Lur'd Leaves has 21.8 total DTs, 9.8 specialized DTs, and 0.8 mine types. Daiye Spa has much higher damage diversity, with 33.7 total DTs, 20.7 specialized ones, and 4.9 mine types. Hubble Bubble shows a maximum damage diversity of 37 total DTs, 21.8 specialized DTs, and 6.4 mine types. This PETM site also has a greater frequency of damage on individual leaves than the older sites.

These sites record the influence of warming on a late phase of terrestrial ecosystem recovery from the K-T extinction. Plants and insects in neighboring North Dakota had high extinction rates, leading to a decrease in diversity of specialized damage types.³ The PETM Hubble Bubble flora is the first North American occurrence of abundant and rich insect herbivory on diverse host plants following the K-T event. The increased herbivory on this thermophilic flora is also consistent with modern ecological studies suggesting that raising temperature increases the abundance and diversity of insect herbivores.

1. J. Zachos *et al*, 2001. *Science* 292: 686-93.

2. C. Labandeira *et al*, 2004. Field guide to insect damage types on compressed fossil leaves, v 1.5.

3. C. Labandeira *et al*, 2002. *PNAS* 99: 2061-6.

MECHANICS OF MIDDLE-GROUND BAR FORMATION: IMPLICATIONS FOR THE MORPHODYNAMICS OF DELTA CHANNEL NETWORKS

Doug Edmonds

Advisor: Rudy Slingerland

Masters Talk

Here we present topological data collected from eleven river-dominated deltas worldwide and explain those data with a three-dimensional numerical model of a middle-ground bar channel levee system. Network topology data exhibit a nonlinear decrease in channel widths, depths, and lengths with increasing bifurcation order. The trends in channel width and depths are an outcome of hydraulic geometry scaling. To understand the trend in channel lengths the mechanics of middle-ground bar formation must be known because bifurcation positions in delta networks are fossilized locations of bars in front of distributary channels. Numerical modeling results, using DELFT3D, show that middle-ground bars form at commencement of turbulent jet expansion because there is increased sedimentation due to rapid expansion. The presence of the middle-ground bar changes the sediment flux slope over the bar and the net result is bar progradation basinward. Bar progradation stops when the depth over the bar is forty-percent of the inlet depth. At this point the pressure caused by fluid piling up against the bar is large enough to divert flow around the bar, rather than over. We have derived a relationship where the distance to middle-ground bar stagnation is a function of jet momentum flux relative to unit area grain weight to the one-fifth power. A multivariate regression indicates that the important variables within that relationship are channel depth and velocity. This relationship can be used to predict width, depth, and length, of future delta channels.

EXAMINING THE MANTLE TRANSITION ZONE BENEATH THE TRANSANTARCTIC MOUNTAINS FROM RECEIVER FUNCTIONS USING TAMSEIS

Mouse Marie Larson

Advisor: Andy Nyblade

Pre-Comps Talk

There is a significant geologic contrast between the East Antarctica Craton (EAC) and the accreted terranes that make up West Antarctica. The boundary between these two provinces is marked by the Transantarctic Mountains (TAM) that parallel the West Antarctica Rift System. The TAM are the largest non-compressional mountain chain in the world, but their origin is not fully understood. Also not well explained is the anomalously high topography of the EAC. A potential cause for both is a thermal upwelling, either a very broad (>500 km wide) anomaly or a narrower one (~100-200 km wide). To investigate these two unique tectonic features of the Antarctic continent, receiver-function stacking is being conducted with broadband seismic data collected by the 2000-2003 Transantarctic Mountain Seismic Experiment (TAMSEIS) to image topography on the 410 and 660 km discontinuities and quantify the thickness of the transition zone. A deep-seated mantle thermal anomaly would evidence itself by creating topography on the 410 and/or 660 km discontinuities. After generating the receiver functions using a frequency-domain deconvolution with water-level stabilization, a geographical binning technique has been applied to better resolve lateral variations in structure. Preliminary results using only Ps conversions from P arrivals and stacking with a 3D velocity model suggest that the transition zone may be thicker than average, with an average 410 but a deeper than normal 660 km discontinuity. The addition of Ps conversions from PP arrivals should improve the quality of the stacks and allow us to image the discontinuities more definitively beneath the study area.

QUANTITATIVE EVALUATION OF H₂S ERUPTIONS FROM THE END-PERMIAN OCEAN

Katja Meyer

Advisor: Lee Kump

Pre-Comps Talk

The cause of the end-Permian mass extinction, the largest extinction event of the Phanerozoic, remains controversial. The role of hydrogen sulfide poisoning has recently become of interest based on biomarker evidence for sulfide in the photic zone of the Permian ocean and biogeochemical calculations by Kump *et al.* (2005). In this scenario, low atmospheric oxygen concentrations, warm surface temperatures and high O₂ demand favored the establishment of euxinia. Catastrophic H₂S release could occur if the upward flux of sulfide from deep-water exceeded the downward flux of oxygen into surface waters. The resulting migration of the chemocline to the air-sea interface would cause sulfide poisoning in both the marine and terrestrial realms. We used GENIE (www.genie.ac.uk), an energy-moisture-balance atmosphere model coupled to a 3-D, non-eddy-resolving, frictional geostrophic model to evaluate this hypothesis. We performed a series of simulations designed to identify the conditions necessary for H₂S outbursts and characterize the magnitude of the fluxes as a function of oceanic phosphate content. Significant ocean-atmosphere fluxes of H₂S result from 6- to 10-fold increases in ocean phosphate at modern oxygen levels. These fluxes are focused in upwelling regions, although toxic H₂S concentrations are also observed in the surface waters of nearshore equatorial regions. Our initial simulations support the hypothesis that episodic H₂S eruptions can result from modest changes in the ocean's nutrient budget and may have contributed to the end-Permian mass extinction. Future work will investigate possible feedbacks involving sulfur utilization by sulfur-oxidizing phototrophs and the role of other nutrients (nitrogen).

FOREARC RESPONSE TO THE MIGRATING PANAMA TRIPLE JUNCTION

Kristin Morell

Advisor: Donald Fisher

Masters Talk

New geologic mapping near the Costa Rica-Panama border reveals a system of structures, surficial deposits and landscape features that are actively propagating to the southeast with the Panama Triple Junction. Near the locus of the triple junction, the northeastward subducting Panama Fracture Zone separates the steeper, slower subduction of the Cocos plate in the west from the more shallow and rapid subduction of the Nazca Plate to the east. As the triple junction migrates along the Middle American Trench at a rate of ~50 km/Ma, the upper plate (Panama Block) of this system experiences an abrupt three-fold increase in convergence rate, and a distinct shallowing in slab dip.

Shallow subduction of the Cocos Plate has led to enhanced subduction-parallel shortening rates in the Fila Costena fold and thrust belt located in the inner forearc of Costa Rica. The thrust belt abruptly terminates to the southeast near the on-land projection of the Panama Fracture Zone, save for a single thrust along the base of the largely undeformed lahar fan derived from the active Volcan Baru. This suggests that the Fila Costena is actively propagating with the triple junction to the southeast, as the upper plate experiences an abrupt shortening increase in the wake of the triple junction. The resultant shortening gradient is partially accommodated by recently discovered right-lateral tear faults found cutting thrusts in the eastern reaches of the Fila Costena. The incipient growth of the thrust belt to the southeast also likely causes the once-consequent and straight rivers draining the forearc to develop curved, subsequence sections, as the topography of the Fila Costena pushes southeastward. Four of the five easternmost rivers of the Fila Costena follow curved paths, including the region's largest river, Rio Chiriqui Viejo, which currently skirts around the eastern termination of the thrust belt. The modern alluvial fan draining the Chiriqui V. drapes atop an older relic fan, the apex of which is located west of the river's current location, suggesting that the river has shifted eastward through time. Additionally, the now-extinct Talamancas arc probably became inactive coincident with a shallowing benioff zone that accompanied the passing triple junction. This resulted in a progressive eastward extinction of the Central American volcanic arc throughout the past ~5 Ma.

CAN HYDROGEOPHYSICAL TOOLS BE USED TO IMAGE BIOGEOCHEMICAL REACTION RATES IN THE SUBSURFACE?

Aaron Regberg

Advisors: Susan Brantley, Kamini Singha

Pre-Comps Talk

Groundwater pollution is and has been a serious problem in our society for many years. There is a whole host of available geochemical and hydrological techniques available for monitoring pollutant plumes, but many of these techniques are costly, provide a limited amount of data, and cannot yield time course information in real time. Almost all available sampling methods require drilling numerous monitoring wells that may themselves affect the calculated properties of the aquifer. Furthermore, sampling these wells only allows geochemical analysis of a small number of points in space and time. Geophysical techniques may provide a way around this. Recently, both electrical resistivity and induced polarization have been used to map the depth and spatial extent of pollutant plumes from sources as diverse as landfill leachate and petroleum spills. It is our hypothesis that geochemical and biogeochemical effects like redox changes, variations in total dissolved solids, and bacterial activity can be quantifiably linked to an electrical geophysical response. We will test this hypothesis by combining bench and column scale experiments with an exhaustive field-scale electrical survey at the Massachusetts Military Reservation (MMR).

The MMR is a USGS toxics field site that has been extensively studied. A nitrate-rich sewage plume has been present at this site for over 50 years. There are numerous multi-level sampling wells and the hydrologic properties are impeccably constrained. Several redox zones have already been identified in and around this plume as well as an area where dissimilatory iron reduction may be occurring. We will attempt to model these processes in the lab to assess the geophysical response to constrained biogeochemical variations. This should allow us to accurately measure and report what is occurring at the MMR.

DEFORMATION OF THE PANAMA MICROPLATE IN RESPONSE TO AN ABRUPT INCREASE IN PLATE BOUNDARY COUPLING

Jason Sitchler

Advisor: Donald Fisher

Pre-Comps Talk

Costa Rica encompasses the forearc and magmatic arc associated with northeast subduction of the Cocos plate beneath the Panama microplate along the Middle America Trench. Dramatic changes in subduction geometry, convergence rate, and upper plate shortening occur in the vicinity of the Panama triple junction (PTJ) where the Panama Fracture Zone (PFZ), separating the Cocos and Nazca plates, subducts orthogonally beneath the Panama microplate south of the Costa Rica-Panama border. There is an abrupt increase in subduction angle from west to east across the PFZ, with shallow subduction of the Cocos plate to the west and steep subduction of the Nazca plate to the east. There is also a sudden decrease in convergence rate from ~80 mm/yr to ~20 mm/yr across the subducting PFZ due to the dextral sense of relative motion between the Cocos and Nazca plates. Consequently, from west to east on the upper plate (i.e. the Panama microplate), there are distinct changes in two tectonic characteristics that coincide with this decrease in convergence rate and increase in subduction angle. These are 1) The lateral termination of the inner forearc thrust belt, related to rough subduction of the Cocos plate, and 2) A change from inactive, exhumed arc in Costa Rica (Cordillera Talamanca) to an active arc in Panama. With regard to the former, we quantified the long-term rates of shortening in the inner forearc thrust belt in southern Costa Rica using balanced cross sections in order to better understand how bathymetric asperities such as the Cocos Ridge can affect plate coupling and upper plate deformation. We estimated that the thrust belt should be accommodating nearly 50% of Cocos-Panama convergence over the long-term. Norabuena and others (2004) also examined the degree of plate coupling along the Costa Rican margin by deploying a GPS survey. Their data, although sparse in the vicinity of the PTJ, indicate a great deal of locking at the boundary in eastern Costa Rica, and contrary to the long-term signal, they show little or no interseismic shortening across the inner forearc thrust belt. However, the data do show a large difference across the cordillera that suggests interseismic strain is accumulating between the forearc thrust belt and the backarc. Little is known about the timing and distribution of uplift in the Cordillera Talamanca. Our next project will focus on these aspects using information gathered from river profiles for the long-term signal of uplift. We also intend to expand the GPS network to include the two areas of greatest tectonic change as discussed above and gain further information regarding the interseismic period. We have extracted longitudinal river profiles from watersheds that drain toward the backarc of the Cordillera. Preliminary data indicate at least one major knickpoint in the upper reaches of streams in all of the sampled watersheds. These knickpoints generally separate the streams into a low-steepness upper section and a relatively high-steepness lower section. We hypothesize that the upper section represents a quasi-steady state profile that formed before uplift of the cordillera, and that the lower section has been incised in response to that uplift.

POSTER PRESENTATIONS – THURSDAY AFTERNOON

<u>Presenter</u>	<u>Advisor</u>	<u>Title</u>
Matthew Bachmann	Lee Kump	QUANTIFYING DENITRIFICATION RATES IN CONTAMINATED AQUIFERS USING qRT-PCR
David Bevacqua	Hiroshi Ohmoto	ORIGIN OF HEMATITE IN THE 3.46GA TOWERS FORMATION
Heather Buss	Susan Brantley	THE COUPLING OF BIOLOGICAL IRON CYCLING AND MINERAL WEATHERING DURING SAPROLITE FORMATION, LUQUILLO MOUNTAINS, PUERTO RICO
Aaron Diefendorf	Katherine Freeman	CARBON ISOTOPES OF LAKE SEDIMENTS INFLUENCED BY BEDROCK AND TERRESTRIAL VEGETATION DURING THE LATE GLACIAL AND EARLY HOLOCENE: A MULTIPROXY STUDY OF LACUSTRINE SEDIMENTS AT LOUGH INCHQUIN, WESTERN IRELAND
Tony Gilman	Donald Fisher	SOUTHEAST DIRECTED THRUSTING ASSOCIATED WITH THE LEADING EDGE OF THE WRANGELLIA COMPOSITE TERRANE: THE CHULITNA BLOCK SOUTH CENTRAL ALASKA
Elisabeth Hausrath	Susan Brantley	BASALT AND GRANITE DISSOLUTION RATES IN THE PRESENCE OF CITRATE
Gavin Hayes	Kevin Furlong	THE EVOLUTION OF A PLATE BOUNDARY SYSTEM - CRUSTAL STRUCTURE AND SEISMICITY IN NORTHERN CALIFORNIA
Bryn Kimball	Susan Brantley, Jennifer Macalady	INVESTIGATING THE COPPER ISOTOPE COMPOSITION OF RED MOUNTAIN CREEK: A STREAM AFFECTED BY ACID MINE DRAINAGE
Victoria Miller	Barry Voight, Charles Ammon	PRECISE HYPOCENTER LOCATION OF HIGH FREQUENCY ONSET EARTHQUAKES AND CHANGING STRESS CONDITIONS BENEATH SOUFRIÈRE HILLS VOLCANO, MONTSERRAT
Tsubasa Otake	Hiroshi Ohmoto	NON-REDOX TRANSFORMATION OF MAGNETITE - HEMATITE UNDER H ₂ -RICH HYDROTHERMAL CONDITIONS
Irene Schneider	James Kasting, Jennifer Macalady	AN ASTROBIOLOGICAL EVOLUTION OF MARS WITH A FOCUS ON ITS RADIATION ENVIRONMENT'
Paul Winberry	Sridhar Anandakrishnan	BASAL MECHANICS OF ICE STREAM STICK-SLIP

QUANTIFYING DENITRIFICATION RATES IN CONTAMINATED AQUIFERS USING qRT-PCR

Matthew Bachmann
Advisor: Lee Kump

Nitrate is the most widespread groundwater contaminant of concern to public health, and the most common pollutant in drinking water supplies. It is also one of the substances most readily removed by native soil microorganisms. Monitoring the rate at which this process occurs is vital to predicting nutrient loading rates to sensitive environments and to keeping our drinking water supplies safe. Here I present a novel method of measuring subsurface denitrification rates using a new molecular technique.

Quantifiable levels of expressed functional genes may serve as proxies for rates of the reactions facilitated by those gene products. In this study, the rate of denitrification by subsurface microorganisms has been correlated with expression levels of the rate limiting nitrite reductase gene *nirS*. The technique uses the Real-Time Quantitative Polymerase Chain Reaction (RT-qPCR) to measure the number of copies of the *nirS* gene expressed in a sample, and correlates that level with known denitrification rates in a laboratory setting to build a calibration curve that can then be applied to environmental samples.

This technique bypasses many of the usual limitations of quantifying subsurface microbial respiration rates. It does not depend on the diffusion of any substance to an active site, has no need of recovery of tracers, and can measure an instantaneous rate on a single sample of a solid matrix or extracted pore water without the need for repeated sampling.

For the purposes of this study, the model organism *Paracoccus denitrificans* was grown in anaerobic batch culture on defined media. Denitrification rates were determined by mass balance of nitrate depletion, and RT-qPCR was carried out using primers and fluorogenic probes specifically designed for the *nirS* gene. Nitrate depletion was measured as a function of temperature and concentration to test the robustness of correlation between gene expression and denitrification rate under varying conditions.

ORIGIN OF HEMATITE IN THE 3.46GA TOWERS FORMATION

David Cicero Bevacqua
Advisor: Hiroshi Ohmoto

The Towers formation (3.46Ga) includes jasper that contains abundant (~6 wt% Fe₂O₃) fine-grained (<1μm) hematite. The presence of hematite (an oxidized iron mineral) is enigmatic because it predates the conventional timing for the rise of oxygen on Earth. It may be a secondary alteration product from the oxidation of primary siderite (a reduced iron mineral) or a primary precipitate from the oxidation of reduced iron in the 3.46 Ga oceans. If primary the reduced iron could have been oxidized by: (i) oxygen produced from the photolysis of H₂O, (ii) the metabolism of phototrophic iron oxidizing bacteria, (iii) oxygen locally produced by cyanobacteria, or (iv) O₂-rich deep ocean water. These possibilities have been discriminated using a holistic geological analysis of Archean Biosphere Drilling Program (ABDP) drill core #1, retrieved from the Towers formation at Marble Bar, Western Australia in 2003. In our study, special attention was given to both large and small features of the cherts (stratigraphy, sediment deformations and formation geometry), microscopic mineralogical characteristics (grain size, distribution, morphology, texture and paragenesis of minerals); and geochemical characteristics (major-, trace- and REE elemental ratios). Our observations support (iv), that hematite is primary and was precipitated locally in >500m of water from rapid mixing of metal and sulfide rich hydrothermal fluids (~250°C) with oxygenated seawater.

THE COUPLING OF BIOLOGICAL IRON CYCLING AND MINERAL WEATHERING DURING SAPROLITE FORMATION, LUQUILLO MOUNTAINS, PUERTO RICO

Heather Buss

Advisor: Susan Brantley,

Corestones of quartz diorite bedrock in the Rio Icacos watershed in Puerto Rico weather spheroidally to form concentric sets of partially weathered rock layers (referred to here as rindlets) that slowly transform to saprolite. The rindlet zone (0.2-2 m thick) is overlain by saprolite (2-8 m) topped by soil (0.5-1 m). With the objective of understanding interactions between weathering, substrate availability and resident microorganisms, we made geochemical and microbiological measurements as a function of depth in 5 m of regolith (soil + saprolite). We employed direct microscopic counting of total cell densities; enumeration of culturable aerobic heterotrophs; extraction of microbial DNA for yield calculations; and biochemical tests for iron-oxidizing bacteria. Total cell densities, which ranged from 2.5×10^6 to $1.6 \times 10^{10} \text{ g}^{-1}$ regolith, were higher than 10^8 g^{-1} at three depths: in the upper 1 m, at 2.1 m, and between 3.7-4.9 m, just above the rindlet zone. High proportions of inactive or unculturable cells were indicated throughout the profile by very low percentages of culturable heterotrophs (0.0004% to 0.02% of total cell densities). The observed increases in total and culturable cells and DNA yields at lower depths were not correlated with organic carbon or total iron but were correlated with moisture and HCl-extractable iron. Biochemical tests for aerobic iron-oxidizers were also positive at 0.15-0.6 m, at 2.1-2.4 m, and at 4.9 m depths. To interpret microbial populations within the context of weathering reactions, we developed a model for estimating growth rates of lithoautotrophs and heterotrophs based on measured substrate fluxes. The calculations and observations are consistent with a model wherein electron donor flux driving bacterial growth at the saprolite-bedrock interface is dominated by Fe(II) and where autotrophic iron-oxidizing bacteria support the heterotrophic population and contribute to bedrock disaggregation and saprolite formation.

CARBON ISOTOPES OF LAKE SEDIMENTS INFLUENCED BY BEDROCK AND TERRESTRIAL VEGETATION DURING THE LATE GLACIAL AND EARLY HOLOCENE: A MULTIPROXY STUDY OF LACUSTRINE SEDIMENTS AT LOUGH INCHQUIN, WESTERN IRELAND

Aaron Diefendorf

Advisor: Katherine Freeman

A 7.6-m lake sediment core from a marl lake, Lough Inchiquin, records variation in landscape evolution from 16,800 to 5,540 cal yrs B.P. Carbon isotope values of calcite and bulk organic material were determined along with total organic carbon, total nitrogen, C/N ratios, total organic matter, and total calcite. We observe significant variations (up to 12‰) in $\delta^{13}\text{C}_{\text{org}}$ and $\delta^{13}\text{C}_{\text{calcite}}$ values that are interpreted to reflect secular changes in the lake water $\delta^{13}\text{C}_{\text{DIC}}$ values as a result of regional landscape evolution from barren limestone bedrock to a forested ecosystem. Lake water $\delta^{13}\text{C}_{\text{DIC}}$ values are therefore influenced by two isotopically distinct sources of carbon: terrestrial organic material (-27.1 to -31.2‰VPDB) via soil CO_2 and weathered limestone bedrock (+3.4‰VPDB). Isotope excursions in lacustrine sediment records are forced not only by changes in productivity but also by changes in the terrestrial environment. This has profound implications for developing paleoclimate records from lacustrine sediment and suggests that selection of appropriate lakes can result in paleoclimate records of terrestrial evolution where other terrestrial records are not available.

SOUTHEAST DIRECTED THRUSTING ASSOCIATED WITH THE LEADING EDGE OF THE WRANGELLIA COMPOSITE TERRANE: THE CHULITNA BLOCK SOUTH CENTRAL ALASKA

Tony Gilman

Advisor: Donald Fisher

Structural mapping of the Chulitna block in south central Alaska reveals a regional scale southeast-vergent, anticline-syncline pair and a series of related southeast-directed thrusts that record the imbrication of the leading edge of the Wrangellia Composite terrane (WCT). The Chulitna terrane has been recognized as an unusual Paleozoic through Mesozoic collage of oceanic and clastic rocks that are not found anywhere else in Alaska or the North American Cordillera. The Chulitna block lies between and divides two basins of the Kahiltna Assemblage flysch (Alaska Range Basin and Talkeetna Mountains Basin) of North American and Wrangellia affinities, respectively. Southeast vergence along the leading edge of the WCT contrasts with the northwest-directed thrusting that typifies the outboard margin of the Talkeetna mountains to the east. Along the southeast margin of the Chulitna terrane, the presence of an accretionary prism with sand-shale mélange, olistostroms, radiolarian chert (the Broad Pass terrane) and deformation of the Chulitna block are consistent with northwest-directed subduction. These data provide kinematic constraints on a new tectonic model for interpreting processes between the Mesozoic margin of North America and the Wrangellia Composite terrane.

BASALT AND GRANITE DISSOLUTION RATES IN THE PRESENCE OF CITRATE

Elisabeth Hausrath

Advisor: Susan Brantley

Bacteria, fungi, lichen and plants all produce organic acids, which can strongly affect weathering by increasing the solubility and mobility of elements. Leaching by organic acids may produce trace element signatures which could record the presence of life.

To determine the effect of organic acid on rock dissolution, powdered Columbia River basalt, and Half-Dome granite Tuolumne River Series sampled in Yosemite National Park were dissolved in the presence of 0.01 M citrate and deionized water in long-term column dissolution experiments. In previous experiments, citrate significantly enhanced element mobilization from basalt. The pH of the input solutions was adjusted to 6, and sodium azide or lithium azide was added to prevent microbial growth. Two empty columns were also eluted with identical inlet solutions (with and without citrate) as controls.

Preliminary results indicate that the elements Ca, Mg, Si, Fe, Al, Sr, Y, Zr, La, Ce, W, Th, P, Sc, Ti, V, Cr, Mn, Co, Ni, and Zn may be leached from the basalt to a greater extent in the presence of the citrate as compared to the ligand-free solution. Na, Mg, Ca, Al, P, Ti, Mn, Fe, Y, La, Ce, Th and Si may be leached from the granite to a greater extent in the presence of the citrate as compared to the ligand-free solution. Further work is needed to quantify and better understand this effect, but these results indicate that organic acids may significantly affect the weathering rates of granite and basalt in natural environments, and the trace element signatures of these rocks after weathering.

THE EVOLUTION OF A PLATE BOUNDARY SYSTEM – CRUSTAL STRUCTURE AND SEISMICITY IN NORTHERN CALIFORNIA

Gavin Hayes

Advisor: Kevin Furlong

The Pacific-North America plate boundary system has developed in response to the northward migration of the Mendocino triple junction through northern California over the past 10-15 million years. Related changes in plate geometry have created the major faults and drive deformation and volcanism in the crust. How a fault behaves in the future is dictated by how that fault evolved. The Ma'acama, Rodgers Creek and Hayward Fault corridor form a major part of this plate boundary system, and reflect its northward evolution, so we can use processes occurring in and on the Ma'acama fault to understand how the Hayward fault evolved in the past, and thus explain its characteristics today.

The Ma'acama fault exhibits the majority of seismic activity in the northern Coast Ranges, and is well defined at the surface through Willits Valley via trenching, paleoseismology and creep analyses. Enigmatically though, precise earthquake relocations reveal that the microseismicity is offset to the east, defining an almost vertical structure up to 10km away from the mapped surface trace of the fault. This disconnect has significant implications for the characteristics and dynamics of faulting in northern California, along what ultimately becomes the dominant plate boundary structure through central California further south. Understanding how this system has developed in the past can therefore help explain how it might act in the future.

INVESTIGATING THE COPPER ISOTOPE COMPOSITION OF RED MOUNTAIN CREEK: A STREAM AFFECTED BY ACID MINE DRAINAGE

Bryn Kimball

Advisors: Susan Brantley and Jennifer Macalady

Acid mine drainage (AMD) is a chronic environmental problem that involves the production of acid from oxidative sulfide mineral dissolution, the transport of acidic, metal-rich waters through ecosystems, and the ultimate neutralization of acidity and attenuation of metals. A better understanding of abiotic and biotic AMD processes is crucial for predicting the fate and transport of metals in the environment and will aid in future remediation efforts. Using a new technique to address this problem, we measured the $^{65}\text{Cu}/^{63}\text{Cu}$ ratios in filtered (pore size = $0.45\mu\text{m}$ or $0.22\mu\text{m}$) samples of AMD-impacted streamwater collected from Red Mountain Creek near Ouray, Colorado. Red Mountain Creek is a small mountain stream receiving metal-rich, acidic drainage from acid-sulfate and quartz-sericite-pyrite alteration zones within dacitic-andesitic lavas and volcanoclastic sediments. We measured $\delta^{65}\text{Cu}$ values [where $\delta^{65}\text{Cu} = ((^{65}\text{Cu}/^{63}\text{Cu}_{\text{sample}}/^{65}\text{Cu}/^{63}\text{Cu}_{\text{standard}}) - 1) \times 10^3$] with a multi-collector inductively coupled plasma mass spectrometer, correcting for instrumental mass bias by doping with the Johnson-Matthey Zn solution and bracketing with the NIST 976 Cu standard. All samples are isotopically enriched in ^{65}Cu relative to the NIST 976 Cu standard, with $\delta^{65}\text{Cu}$ values ranging from $1.03 \pm 0.10\text{‰}$ to $3.76 \pm 0.10\text{‰}$ (2σ). The most isotopically enriched sample is of an inflow emanating from a mineshaft that displays the highest Cu concentration (10.4 mg/L). The $\delta^{65}\text{Cu}$ values of filtered streamwater decrease downstream, coincident with decreasing Cu concentration and increasing pH. Thus, an isotope effect (whereby ^{65}Cu is preferred) may be associated with processes that remove Cu from streamwater, such as sorption and microbial interaction. These field results agree with previous experiments where Cu associated with *Acidithiobacillus ferrooxidans* cells was isotopically enriched in ^{65}Cu after 30 days relative to dissolved Cu in the original growth medium. Future experiments will aim to tease apart the processes contributing to the cumulative Cu isotope fractionation measured in AMD-impacted streamwater. Specifically, we will test whether Cu isotopes are fractionated during sorption to ferric oxide minerals and during interaction of aqueous Cu with microorganisms. Such experiments will provide insight into the abiotic and biotic mechanisms that control the mobility of Cu, and other metals, in environments contaminated with toxic AMD.

CRUSTAL THICKNESS AND POISSON'S RATIO OF CONTINENTAL CRUST

Minoo Kosarian

Advisor: Charles Ammon

An important component to the understanding the evolution of the continental lithosphere is to improve our knowledge on lower continental composition. Contribution towards this goal, we perform receiver function analysis using teleseismic waveforms recorded at permanent and temporary broadband seismic stations located in Middle East, Europe, Asia, and north Africa. Two hundred and twenty six stations recording a total of about 6,000 teleseismic events producing more than 100,000 seismograms have been investigated. The distribution includes 72 stations in the Middle East, 57 stations in Europe, 60 stations in Asia, and 37 stations in central and north Africa. We have examined receiver functions for 213 of stations (selection of best data) in the period of 1990-2004 and applied the receiver function stacking procedure of Zhu and Kanamori [2000] to estimate Poisson's ratio and crustal thickness. We have divided the research area according to five tectonics environments, explicitly Shields, Platform, Paleozoic orogenic belts, Mesozoic-Cenozoic orogenic belts, and rift zones based on Condie's [1989] simplified classifications. The results from this study shows lower value of Poisson's ratio $s=0.25$ for Shield and Platform compare to the Orogenic-belts with $s=0.27$. Crustal thickness for Shield and Platform show the value of 38km and 43km respectively, while for the Orogenic belts we found a value of 37km for Paleozoic belts and 39km for Mesozoic-Cenozoic belts, although the range of thicknesses for the younger active regions is large. Since our ultimate goal is to provide an improved imaged of global continental structure and composition, we combine our observations with receiver functions results from other published analysis. In total we have integrated observations from 374 stations located in different geologic setting and the results indicate the value of $s=0.26$ for Poisson's ratio and $H=38\text{km}$ for crustal thickness in Shield, $s=0.27$ with $H=43\text{km}$ for the Platform, and $s=0.28$ with $H=36\text{-}39\text{km}$ for the Orogenic belts. We will compare crustal thickness and Poisson's ratio estimates for the crust beneath the stations with the recent global studies.

PRECISE HYPOCENTER LOCATION OF HIGH FREQUENCY ONSET EARTHQUAKES AND CHANGING STRESS CONDITIONS BENEATH SOUFRIÈRE HILLS VOLCANO, MONTSERRAT

Victoria Miller

Advisors: Barry Voight and Charles Ammon

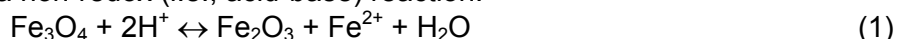
Volcano-tectonic (VT) earthquakes are interpreted as resulting from slip on fractures or faults induced by magma pressurisation. Examination of VT earthquakes can provide information on areas of magma storage and any induced stress state due to such pressurisation. The andesite stratovolcano of Soufrière Hills (SHV), Montserrat, has been intermittently erupting now for 10 years. During the eruption there have been several phases of activity and VT seismicity has varied throughout this period. Here we use the data from Montserrat to more precisely constrain the magma storage and transport system, and stress changes which have occurred during this eruption. Recent developments have allowed more precise hypocenter relocations using relative positioning techniques. Studies using such methods (e.g., Prejean et al., 2002) have demonstrated improvements in location precision, with distinct lineaments emerging where previous techniques had merely identified earthquake clusters. Therefore we have examined seismic data recorded at SHV, utilising the Waldhauser and Ellsworth (2000) precise relocation technique. The aim of the study is to provide clarification of distinct structures that may have influenced magmatic processes. In addition we use these locations to assist with determination of fault plane solutions, which are explored in order to detect any stress changes that have occurred in concert with pulsatory magmatic pressure episodes. Examination of the data for both spatial and temporal patterns provides constraints on magma storage and transport dynamics at SHV. Changes in the localised stress pattern from that of the regionally determined stress regime on a volcano may provide additional information to those monitoring for signs of renewed activity.

NON-REDOX TRANSFORMATION OF MAGNETITE – HEMATITE UNDER H₂-RICH HYDROTHERMAL CONDITIONS

Tsubasa Otake

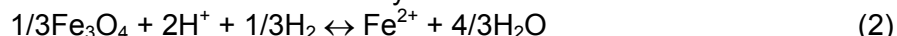
Advisor: Hiroshi Ohmoto

Magnetite (Fe₃O₄) and hematite (Fe₂O₃) are used to constrain the redox conditions of fluid (or melt) from their presence or absence in rocks. Magnetite-rich Banded Iron Formations (BIFs) and secondary hematite-rich iron ore formations have been linked to the oxygenation of the ocean and atmosphere, assuming redox transformation of magnetite – hematite. However, magnetite – hematite transformation may proceed through a non-redox (i.e., acid-base) reaction:



Magnetite is transformed to hematite as a result of leaching Fe²⁺ from magnetite while hematite is transformed to magnetite as a result of incorporating Fe²⁺ into hematite. We have examined the reactions (forward and reverse) using a hydrothermal cell with hydrogen electrodes for pH measurements and a hydrogen-permeable membrane for P_{H₂} measurements. The experiments were conducted at 100 - 250°C under highly reducing conditions (P_{H₂} = 0.5 – 50 bar) and mildly acid conditions (pH = 4 – 6). After the system reached a steady state, iron concentration in the withdrawn sample solutions was measured by ICP-AES. The residual solid was analyzed using XRD, SEM and HRTEM.

Our experiments have demonstrated that euhedral crystals of hexagonal dipyramidal hematite grow rapidly by reaction between magnetite and acid solutions at T ≤ 200 °C, suggesting dissolution and reprecipitation of Fe³⁺ under highly reducing conditions. Rapid dissolution and reprecipitation of Fe³⁺ may be promoted by the presence of Fe²⁺ in the solution through electron transfer and/or indicate the importance of nanoparticle or aqueous Fe₂O₃(aq) for crystallization of hematite. Chemical composition of the experimental solution at the given temperatures are independent of the H₂ pressure and remain constant over weeks, controlled by reaction (1). Reaction (1) is reversible, although the reverse reaction is more sluggish than the forward reaction. However, at T = 250°C, reductive dissolution of magnetite (i.e., redox reaction) controls the chemical compositions of the solution after 4 days:



No hematite was found in the residual solid from experiments at the temperature.

The results of our studies suggest magnetite and hematite act as an acid-base buffer, rather than a redox buffer in low temperature environments. Because magnetite – hematite transformation does not require a redox reaction, secondary hematite-rich iron ore developed from BIFs may have formed by subsurface reaction between magnetite and acidic hydrothermal solutions at T ≤ 200 °C.

'AN ASTROBIOLOGICAL EVOLUTION OF MARS WITH A FOCUS ON ITS RADIATION ENVIRONMENT'

Irene Schneider

Advisors: James Kasting, Jennifer Macalady

The radiation environment on the surface of a terrestrial planet such as Mars is crucial to its potential past and/or present habitability. Despite this, the subject of high energy radiation is rarely contemplated within the field of Astrobiology as an essential factor determining the realistic parameter space for the development and preservation of life.

Furthermore, not much is known of the radiation environment on the surface of Mars due to the fact that no real data exists on this contribution. There are no direct measurements available since no surface landers/probes have ever carried nuclear radiation detection equipment to characterize the interactions arising from cosmic ray bombardment and solar particle events striking the planetary surface. The first mission set to accomplish this precise task, the Mars Science Laboratory, is not scheduled to launch until 2006. In addition to this, recent detection of subsurface hydrogen by the Odyssey spacecraft has prompted an in-depth study of backscattered radiation since hydrogen is a highly effective neutron moderator. Recent simulations utilizing specialized nuclear transport codes developed by NASA are currently producing results showing that this incident as well as scattered contribution might be in fact quite significant and thus must be carefully accounted for.

Presented here are some of such simulations as well as a discussion on the implications that these projected doses would have on terrestrial planet habitability on Mars and elsewhere.

KINETIC ANALYSIS OF COPPER SULFIDE PHASE TRANSITIONS USING TIME-RESOLVED SYNCHROTRON XRD: CHALCOCITE TO COVELLITE

Andy Wall

Advisor: Peter Heaney

Sulfide minerals play an important role in the mobilization, transport, and fate of toxic elements in the environment. The association of sulfides with heavy metals (ie. Cu, Pb, and As), as well as their acid generating propensity during oxidation, underscore the need to investigate the mechanisms of sulfide mineral transformation during dissolution/precipitation, as well as reaction rates in ambient environments. Previous work has demonstrated a phase transition during oxidation of copper sulfides. This study utilizes time-resolved Synchrotron X-ray diffraction (SXRD) to determine the reaction kinetics and structural changes of chalcocite (Cu_2S) transforming to covellite (CuS) during oxidation with ferric sulfate. Intermediate phases include djurleite ($\text{Cu}_{1.94}\text{S}$), digenite ($\text{Cu}_{1.80}\text{S}$), anilite/roxybite ($\text{Cu}_{1.75}\text{S}$), geerite ($\text{Cu}_{1.6}\text{S}$), spionkopite ($\text{Cu}_{1.4}\text{S}$), and yarrowite ($\text{Cu}_{1.13}\text{S}$).

Using flow-through reactors at the National Synchrotron Light Source at Brookhaven National Laboratory, standard grade monoclinic chalcocite was leached with 0.1 M and 0.01 M ferric sulfate with X-ray exposure intervals of 2 minutes. Preliminary results show the timing of the transition from chalcocite to the end-member copper sulfide mineral is ~10 minutes with 0.1M ferric sulfate and ~100 minutes with 0.01M ferric sulfate. While these data are generally consistent with a first order exponential decay reaction models, and agree with previous batch reaction studies, the transition between phases may be better modeled by linear step functions. This suggests that the rate of transition from chalcocite to covellite may be phase dependent. Further work is needed using Rietveld analysis to provide better constraints on the phase abundance throughout the reaction as well as atomic positions.

BASAL MECHANICS OF ICE STREAM STICK-SLIP

Paul Winberry

Advisor: Sridhar Anandakrishnan

The fast-flowing ice streams and outlet glaciers that drain the interiors of large ice sheets are a principle component controlling their mass balance. However, an increasing body of literature is demonstrating that ice streams are not stable features of ice sheets but, exhibit large temporal fluctuations on a wide range of time-scales, complicating how we interpret past and future changes of ice sheets. At the hundred year to millennial time scales ice streams shut-down, restart, and change flow direction. At sub-day scale ice streams velocities fluctuate widely in response to the ocean tides at the grounding line. Understanding how these variations impact the long-term behavior of ice sheets is essential to predicting the evolution of ice sheets and their contributions to future sea-level rise.

Stick-slip motion of Whillans ice stream (WIS) is one of the more surprising observations of the non-steady flow ice stream exhibit. The downstream portion of WIS consists of a wide, > 100 km, ice plain of lightly grounded ice that extends more than 150 km inland from the grounding line. While the WIP moves at typical ice stream velocities, >100 m/yr, it accomplishes most of this motion in short 10-30 minute burst followed relatively long, 6-25 hours, stagnant periods. Stick-slip motion is an unstable phenomenon that complicates traditional views of steady ice stream. WIS is of special interest because it both drains a large portion of the West Antarctic Ice Sheet (WAIS), ??% of the WAIS, and is presently decelerating, possibly stagnating by the end of this century. For this reason, understanding its current deceleration and the future of the WAIS requires a better understanding of ice stream stick-slip motion. We begin addressing the need for a quantitative model of ice stream stick-slip motion by presenting an analysis of ice stream stick-slip mechanics using a recently collected data set on WIS and surrounding regions.